Development of a novel RF body coil integrated with MR-compatible PET detector

Gary H Glover[1], Craig S Levin[1], Anton Linz[2], William T Peterson[2], and Sri Harsha Maramraju[2]
[1]*Stanford University School of Medicine, Stanford, CA, United States,* [2]*GE Healthcare, Waukesha, WI, United States*

Objectives: The hybrid PET/MR prototype from GE Healthcare integrates a high performance Time-of -Flight MR-compatible PET system with a high performance MR scanner for simultaneous PET/MR imaging. The MR system is based on GE's MR750w scanner, while the PET system is designed and developed with MR-compatible detector components to function in the MR environment. In this study, we evaluated the impact of the PET detector ring on the performance of the novel PET/MR RF body coil, which is uniquely designed and constructed to accommodate the PET detector ring integrated with the body coil and residing inside the gradient coil. In addition, the performance of the PET system during active MR acquisition was evaluated.

Methods: The magnet, gradient coil and supporting electronics for the hybrid PET/MR scanner are standard MR750w components. In order for the PET detector ring to be configured entirely on the outside of the RF coil and centered, the new PET/MR body coil design uses an RF shield which dips inward toward the RF conductors in the center portion of the coil as shown in Figure 1. The reduced RF rung-to-shield gap in the center of the body coil provides additional space to accommodate the 25 cm axial PET detector length with a 60 cm patient bore. The performance of the PET/MR RF body coil was evaluated using routine MR pulse sequences and with various MR phantoms to measure B1 field homogeneity, signal-to-noise ratio, image temporal stability and geometric distortion parameters, respectively. All measurements were performed with PET system integrated and under both powered off and on conditions (Figure 2). Furthermore, PET energy and timing resolution measurements were performed during active MR scanning conditions using Ge-68 cylindrical pin sources. In addition, PET sensitivity was measured in the absence of MR scanning,

Results: From initial tests, we observed that there were no visible streak artifacts on MR images when the PET system was simultaneously acquiring data (Figure 3). The B1 field homogeneity of the body coil measured with a silicon oil-filled spherical phantom is maintained even in the presence of the integrated PET system acquiring data. The MR signal-to-noise ratios showed minimal degradation when the PET system was powered on (81.95) compared to PET off condition (89.95). These SNR values were superior compared to that measured separately in a standard MR750w coil design (64.34), with the same phantom. There was no significant degradation in MR images with and without PET powered on, when an ADNI distortion phantom was used to evaluate geometric distortion (Figure 4). Results from image temporal stability measurements (image-to-image repeatability and behavior) infer no degradation with the PET system powered on. During PET system performance evaluation, there was no negative impact on energy resolution with and without RF stimulus (10.5% vs. 10.5 %). The high intensity RF pulses had minimal impact on PET timing resolution (399 ps) compared to no RF stimulus (390 ps), when measured using Ge-68 pin source. The PET NEMA sensitivity measured using Ge-68 line source peaked at 23.83 cps/kBq at center and 23.55 cps/kBq at 10 cm off radius with Compton scatter recovery.

Conclusions: We evaluated the performance of a newly designed RF body coil with integrated PET ring for simultaneous PET/MR imaging. Initial test observations indicate promising MR results with body coil performance in the presence of the integrated PET system. We also evaluated preliminary PET performance with and without RF pulsing, demonstrating feasibility to perform simultaneous multimodal imaging. Further quantitative image quality tests and technical evaluation of overall PET system performance inside and outside the MR environment are under way.

PET/MR RF Body coil

Figure 1. Schematic of RF Body Coil

PET Performance during active MR

	RF OFF	RF ON
Energy Resolution (%)	10.5	10.5
Time Resolution (ps)	390	399

NEMA Sensitivity (PET only)		
Line source centered	23.83	cps/kBq
Line source 10 cm up	23.55	cps/kBq

MR Performance with integrated PET

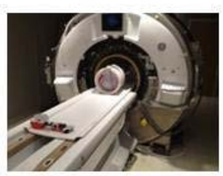

Comparison of MR SNR

	Signal	Noise	SNR
PET/MR Body Coil (PET ON)	2825.1	34.48	81.95
PET/MR Body Coil (PET OFF)	2836.0	31.53	89.95
MR750W Standard Body Coil	1345.4	20.91	64.34

Figure 2. RF Body Coil and PET detectors integrated inside gradient coil

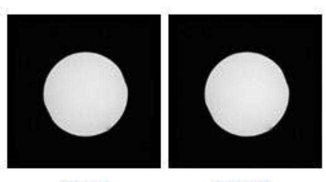

Image Temporal Stability	PET OFF	PET ON
Mean signal intensity	7445.39	7373.78
Signal Intensity Drift (%)	0.045	0.044
Signal-to-fluctuation-noise ratio	335.08	334.68

Figure 3. No visible streaks/artifacts in the MR images with PET powered ON.

Geometric Distortion

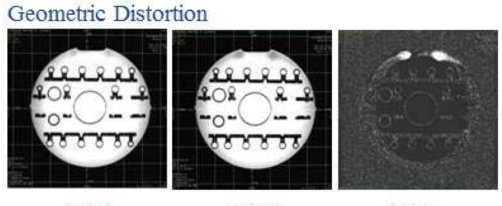

B1 field homogeneity

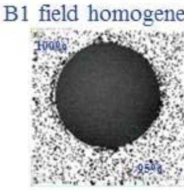

Figure 4. Qualitative evaluation of ADNI Distortion phantom with PET OFF and powered.